

Ultra-Fast Temperature Estimation of Lithium-Ion Batteries Through Impedance Measurements

1st Minh Tran
Electrical Engineering Department
Tampere University
Tampere, Finland
minh.tran@tuni.fi

2nd Daniel Stroe
AAU Energy
Aalborg University
Aalborg, Denmark
daniel.stroe@aau.dk

3rd Tomi Roinila
Electrical Engineering Department
Tampere University
Tampere, Finland
tomi.roinila@tuni.fi

Abstract—Lithium-ion (Li-ion) batteries have become increasingly important in the electrification of transportation and electrical energy production in recent years. Despite the growing popularity, Li-ion batteries face several challenges such as safety hazards and environmental issues from battery waste. Safe and long-lasting battery operation can be achieved by efficiently monitoring and regulating key state parameters such as the cell temperature. However, current temperature estimation methods rely on limited sensing devices and complicated modeling techniques which can be difficult to implement at low cost. Studies have shown a good correlation between the battery impedance and temperature, suggesting that the former can be a suitable indicator for estimating the latter. The recently proposed discrete-interval binary sequence (DIBS) broadband method have been shown to overcome several disadvantages of traditional electrochemical impedance spectroscopy such as long measurement time and costly equipment. This paper demonstrates the use of the DIBS in developing a temperature estimation algorithm for a commercial Li-ion battery cell. Experimental results based on several commercial Li-ion battery cells are presented to demonstrate the effectiveness of the proposed method. An overall estimation accuracy of less than 2 °C absolute error was achieved by applying least square fitting and linear models, thus showing that temperature estimation through cell impedance measurement can be highly effective even when applying simple modeling techniques.

I. INTRODUCTION

The use of Li-ion batteries in transportation and various industrial applications have been continuously rising in recent years. This is due to many high performance properties of Li-ion batteries such as high energy density and long battery life [1]. However, Li-ion batteries have a potential for safety hazards due to thermal runaway. In addition, most Li-ion batteries are being land-filled upon reaching end of life which raise environmental issues. Therefore, Li-ion battery applications require constant monitoring of state parameters such as temperature and state-of-health (SOH) in order to maintain a safe and long-lasting operation while keeping the cost of the battery sufficiently low.

The temperature is an important state parameter which strongly influences the performance of a Li-ion battery. For example, cell operation at too low temperature causes reduced capacity and lithium plating while too high temperature causes accelerated cell degradation. Outside of the safe temperature range (typically between -20 and 60 degrees Celsius), the

battery faces risks of failure and thermal runaway. High variation in temperatures of cells in a battery pack also reduces the performance and life time of the battery. While a practical battery thermal management system can constantly regulate the battery temperature, the use of limited number of conventional temperature sensors is not an efficient method due to relatively high cost and design constraints. Various sensorless temperature estimation methods have been proposed to predict cell-level temperature but most are often complicated and computationally demanding [2].

Studies have shown the effectiveness of the impedance in determining the temperature of a Li-ion battery cell [3]. The impedance is conventionally measured by the electrochemical impedance spectroscopy (EIS) technique in which the battery is injected by sinusoidal excitations at various frequencies and the impedance is estimated by applying Fourier methods to the measured battery voltage and current. While the EIS can accurately and reliably measure the battery impedance, the method is impractical for onboard battery monitoring applications due to long measurement time and challenging hardware implementation.

Recent studies have presented methods based on binary broadband perturbations and Fourier techniques to measure the battery impedance [4]–[6]. In the methods, a binary broadband current is applied to the battery. The resulting output voltage is measured, and Fourier transform is applied to extract the spectral information. The methods make it possible to measure the battery impedance reliably and accurately over a wide frequency band in a fraction of time compared to the conventional EIS.

This paper presents a practical temperature-estimation method for a Li-ion battery using the battery internal impedance obtained by applying a discrete-interval binary sequence (DIBS). The DIBS is a computer-optimized broadband binary signal recently demonstrated as an effective method to measure the battery impedance [7], [8]. Due to the broadband nature and the ability to increase the signal harmonic spectral energy without increasing time-domain amplitude, applying the DIBS excitation in battery impedance measurement produces highly accurate and fast results.

The rest of the paper is organized as follows. Section II gives a theoretical background for battery dynamical states

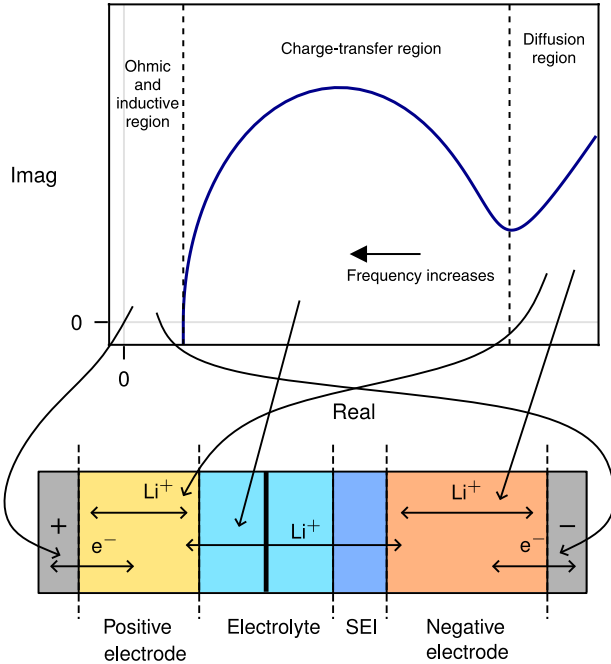


Fig. 1: Li-ion cell internal impedance curve and charge transportation across different cell layers.

characterization based on the internal impedance. Section III describes the methods for battery impedance measurement. Section IV presents experimental measurements based on a commercial Li-ion battery. Section V analyzes the measurement results and perform temperature estimation. Finally, Section VI draws conclusions.

II. THEORY

Studies have shown that the internal impedance provides key information about a Li-ion battery performance [9]. The impedance is typically represented as a complex-value function in the frequency domain as $Z = R + jX$, where R is the real part of the impedance that describes the resistive characteristic and X is the imaginary part of the impedance that describes the reactive characteristic. Fig. 1 shows a typical impedance spectra of a Li-ion battery cell as a Nyquist plot. The imaginary axis is inverted to show the capacitive characteristic in the first quadrant of the diagram. The impedance curve can be divided into several regions that describe the movement of charges at different parts of the cell. At low frequencies of less than a few hundred mHz, a 45° rising line in the impedance curve describes the diffusion of Li-ions in the electrodes. The mid-frequency region, which usually ranges from several mHz to a few kHz, describes the charge transfer of Li-ions in between the solid-electrolyte interphase (SEI) layer, the electrolyte and the electrodes. At higher frequencies, ohmic and inductive behaviors dominate and characterize the electronic flow in the outer conductive parts of the cell.

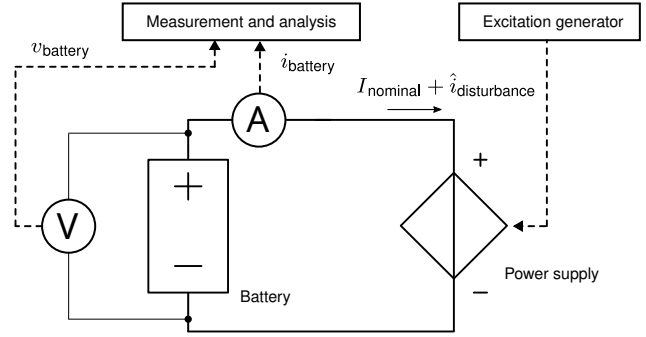


Fig. 2: Battery impedance measurement setup.

The cell internal impedance has a direct relationship with the cell temperature. The cell temperature is an indicator of average thermal kinetic energy which comes from two sources: internal heat generation and external heat absorption. As an electric current flow is applied to the cell during charging or discharging, heat losses occur due to the cell inherent resistive characteristics. However, when the cell receives extra heat either from outside sources or self-heating, Li-ion exchange traffic in the cell is accelerated which in turn decreases the internal impedance of the cell. A thermal equilibrium is reached as the impedance stabilizes indicating a balanced state of heat generation and radiation.

Studies have demonstrated various methods to estimate the battery temperature using the battery internal impedance [10]–[16]. The developed methods employ various mathematical tools such as linear regression, equivalent circuit modeling, thermal modeling and resulted in varying estimation accuracy levels ranging from 0.1 to 7 degrees Celsius absolute error. Estimation accuracy depends on the applied modeling technique and, when applying statistical techniques such as regression analysis and neural networks, the selection of learning features and the sample size.

III. METHODS

A. Battery impedance measurement

Fig. 2 presents the basic principle for measuring the battery impedance. An external power source applies a current disturbance to charge and discharge a battery cell. The current injection produces a voltage response at the cell terminals. Both the cell current and voltage are measured and Fourier transform is applied to obtain the impedance. Multiple injection periods and averaging techniques are typically employed to improve the quality of the result.

A battery impedance is conventionally obtained by applying the EIS [17]. In the EIS, waves of sinusoidal excitation current at multiple frequencies are sequentially injected to the test cell according to Fig. 2. The EIS provides accurate impedance measurement results, but applying sinusoidal excitations requires a relatively long measurement time. Furthermore, sinusoids contain a large number of signal levels, thus

generating such signals is difficult in practice where the cost of implementation must be minimized.

Recent studies have demonstrated methods based on broadband perturbations such as the pseudorandom binary sequence (PRBS) to measure the battery impedance in a fraction of time compared to the EIS [4]–[6]. The PRBS is a popular broadband signal which carries spectral energy at multiple harmonic frequencies. Fig. 3 shows an example PRBS excitation (blue) in both the time domain and the frequency domain. As can be seen, in the time domain the PRBS has only two signal levels which is easy to generate using low-cost electronic devices. In the frequency domain, the signal total energy is uniformly distributed across the spectrum which allows for full spectral coverage of an impedance measurement in a single signal injection. As a result, an impedance measurement applying the PRBS takes only a fraction of time to complete compared to the conventional EIS.

B. Discrete-interval binary sequence

Applying the PRBS in a practical battery impedance measurement faces challenges as the measurement accuracy can be highly sensitive to noise disturbance. This is due to the total PRBS signal energy being distributed to a high number of harmonics in the spectrum. High enough signal-to-noise ratio (SNR) per each harmonic frequency is desirable since the typically low cell impedance value causes the voltage response to be small in amplitude that is highly sensitive to external noise. Increasing the time-domain amplitude increases the signal total energy which improves the SNRs but the linear operating region of the cell impedance can be violated or the nominal system operation can be affected during the measurement.

Recent studies have demonstrated the use of the discrete-interval binary sequence (DIBS) as an alternative to the PRBS for online battery impedance measurement [7], [8]. The DIBS is a computer-optimized broadband signal where the signal power at user-picked harmonics can be amplified without increasing the signal time-domain amplitude. Therefore, compared to the conventional PRBS, the user-specified frequencies of the DIBS have significantly higher signal-to-noise ratios (SNRs) while keeping the same time-domain amplitude. The DIBS carries all the advantages of a conventional PRBS such as low-cost implementation and significantly improved measurement time compared to conventional EIS.

The optimization procedure for synthesizing the DIBS can be summarized as follows [18]–[21].

- 1) Select the sequence length, bandwidth and the amplified frequencies inside the bandwidth.
- 2) Apply a series of optimization iterations.
 - a) Start with a random binary sequence, obtain the phase angle in the frequency domain.
 - b) Form a new sequence by using the phase angle and the user-defined spectral amplitude.
 - c) Apply Inverse Fourier Transform to the newly formed sequence and collect only the signs of

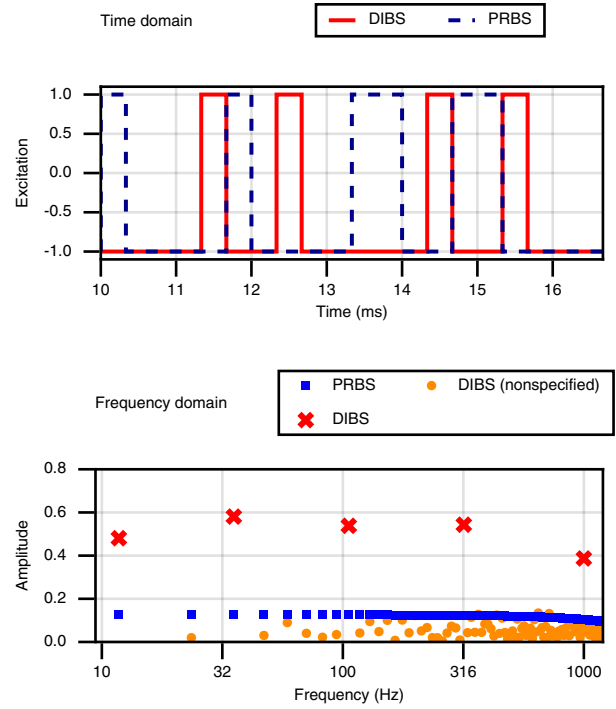


Fig. 3: PRBS and DIBS (5 harmonics) of length 255 and 3 kHz generation frequency in the time domain and frequency domain.

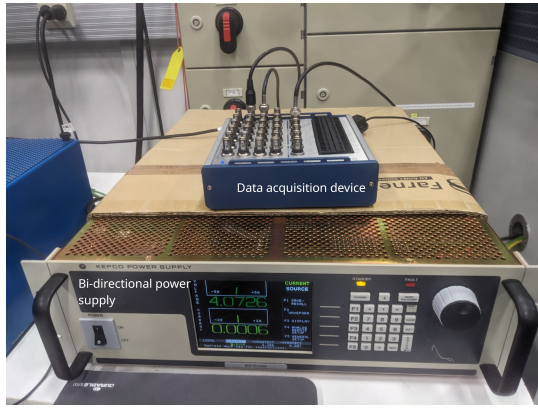
the time-domain sequence in order to form a new binary sequence.

- d) Apply Fourier Transform to the new binary sequence and repeat until the phase angle sequence remains unchanged.

Fig. 3 compares the DIBS and the conventional PRBS in the time and frequency domain. Both sequences (255 bits long) have been generated at 3 kHz and have the same time-domain amplitude. For the DIBS, five harmonic frequencies were logarithmically selected and the signal energy was maximized at these frequencies. The specified DIBS harmonics have approximately five times higher energy level than the PRBS in this example.

IV. EXPERIMENTAL SETUP

An experimental setup based on Fig. 2 was constructed to perform the battery impedance measurement using the proposed method. Fig. 4 shows the setup equipment from the laboratory and a test battery cell placed inside a temperature-controlled test chamber. The impedance of four new commercial Li-ion battery cells (labeled C1, C2, C3, and C4) of the same chemistry and model (i.e., NMC cathode, Samsung INR21700-40T) were measured in order to study the relationship between the battery temperature and impedance. The DIBS was applied to measure the cell impedance in the frequency band 0.1 Hz to 2 kHz at all the test conditions. The



(a) Data acquisition device and bi-directional power supply.



(b) NMC-based Li-ion battery cell placed in the climatic chamber.

Fig. 4: Experimental setup.

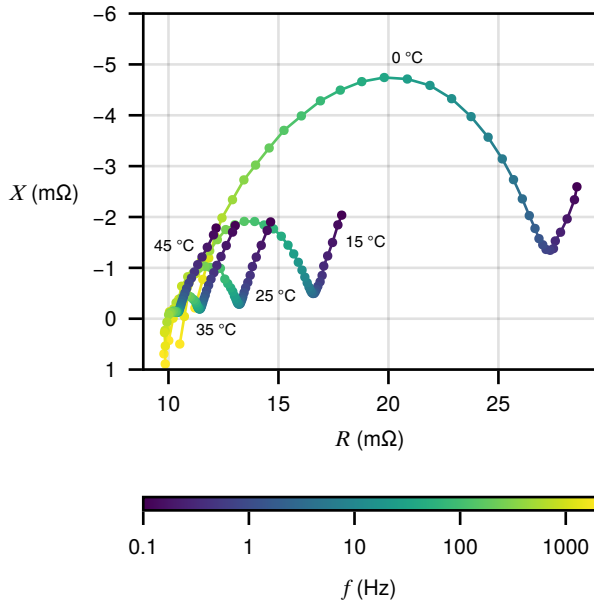


Fig. 5: Battery impedance spectra of cell C4 measured with the DIBS technique at various temperatures and 80% SOC.

excitation amplitude was selected as 250 mA at which value the disturbance is sufficiently small while providing enough signal-to-noise ratios for the measurement. The speed of the measurement equals to the time period of the lowest frequency. Hence with 3 periods of injection and at 0.1 Hz lowest frequency, each measurement took about 30 seconds to complete. On the other hand, an EIS measuring an equivalent frequency band takes up to 5 minutes to measure. The impedance of the cells were measured at various temperatures (0, 15, 25, 35, 45 degrees Celsius) and at various SOC from 20% to 80%. The cell temperature setpoint was reached by relaxing the cell in a temperature-controlled climatic chamber for two hours prior to each measurement. Fig. 5 shows the impedance measurements of a single cell at 80% SOC at the specified temperatures.

V. TEMPERATURE ESTIMATION

A. Regression analysis

A regression analysis was applied to the experimental measurement results to study the relationship between the specified temperature values and the measured cell impedance. In regression analysis, a regression model is chosen where its parameters can be estimated by fitting the training dataset to the model via an optimization method, such as the least-square method. The fitted model can then be used as an estimator on the testing dataset, in which an estimation of temperature can be produced from an impedance measurement of a test cell. The estimation is compared against the reference temperature measurement to evaluate the regression accuracy. The regression analysis process applied in this work consists of the following steps.

- Collect experimental impedance measurement results.
- Extract input features from the impedance value at each frequency of each cell.
- Apply the least-square method to the input features of the training dataset to obtain the regression model parameters at each frequency.
- For each frequency, compute the average model parameters from all the cells.
- Evaluate the obtained averaged models accuracy by self-validation, in which each cell in the training dataset becomes a test cell and the estimation error is calculated for each cell at each frequency.
- Find a range of frequencies in which the validation metric values satisfy a set of predefined criteria to obtain a set of optimal estimators.
- Use the obtained estimators to estimate the cell temperature using impedance measurement from the test dataset and compute the estimation errors.

B. Linear regression

A simple linear regression analysis was first applied to the experimental results obtained for all the cells at 80% SOC at the specified temperatures (0°C → 45°C). The real part of the impedance at each frequency was used as the input feature in the analysis. A linear model describing the relationship between the real part of the measured cell impedance, denoted

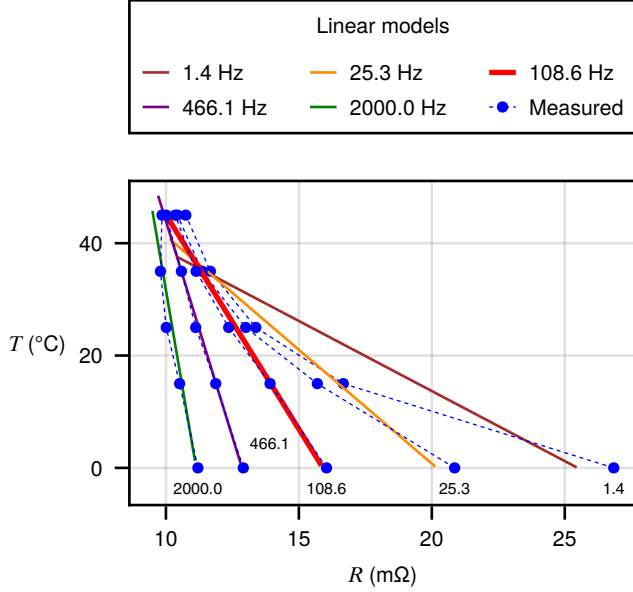


Fig. 6: Linear model fitting between the cell temperature and the real part of the measured impedance at various frequencies of cell C4 at 80% SOC.

Temperature	Linear regression	Quadratic regression
0 °C	2.39 °C	0.77 °C
15 °C	2.39 °C	1.81 °C
25 °C	3.42 °C	2.43 °C
35 °C	2.9 °C	2.61 °C
45 °C	0.28 °C	0.91 °C

TABLE I: Estimation errors of regression methods at various temperatures.

as R , and the cell temperature, denoted as T , is formulated as $\hat{T} = \beta R + \epsilon$ where β and ϵ are the linear coefficients per harmonic frequency in the spectrum and \hat{T} is the estimated temperature value. The measured impedance of each cell in the training dataset consisting of cells C2, C3, C4 was fitted to produce linear models at various frequencies. Fig. 6 shows the fitted linear models between a cell temperature and the real part of the cell impedance at various frequencies. The figure shows that at some range of frequencies, the temperature value (dashed lines) is highly linearly correlated to the real part of the measured impedance.

The coefficient of determination R^2 which describes the fidelity of a linear regression model on a dataset was used to evaluate the performance of the fitted linear regression models. In addition to R^2 , the root-mean-square error (RMSE) was also used to assess the regression performance. Fig. 7 shows the R^2 index values and RMSEs at various frequencies of each cell in the training set validated against their own measurement data. By selecting a minimum value of 0.97 for R^2 and a maximum

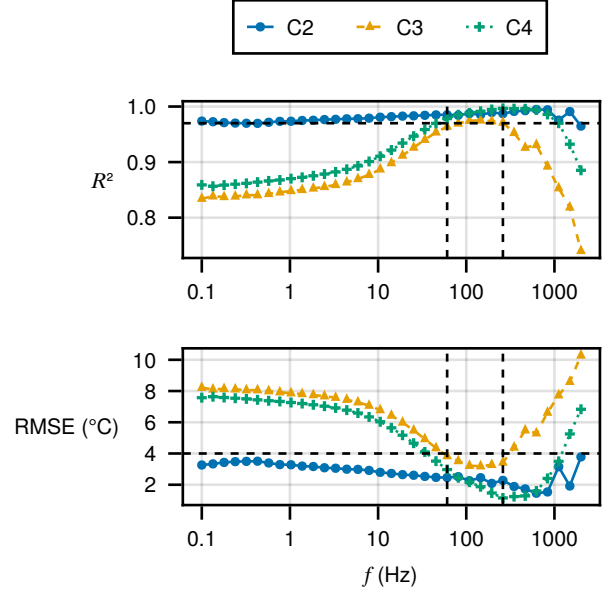


Fig. 7: Linear regression performance by self validation.

value of 4 °C for RMSE, a range of frequencies between 60 Hz and 260 Hz were identified as potentially accurate estimators of temperature. For each frequency in the identified range, averaged parameters were obtained by calculating the average of model parameters from all the cells. The obtained set of models based on averaged parameters were used as the results of the model training process.

The estimators obtained from the training phase were used to estimate the temperature of test cell C1 the impedance of which was measured at 80% SOC and at the specified temperatures. For each measurement, the real part of the measured impedance values at various frequencies were used as the input to the estimators. The estimation value obtained from each frequency are then averaged to produce the final temperature estimation value. The estimation errors were calculated by calculating the absolute difference between the estimated and the reference temperature values $\Delta\hat{T} = |\hat{T} - T|$. Table I summarizes the estimation errors for each temperature. On average, linear regression produces an estimation error of about 2.18 °C.

C. Quadratic regression

The nonlinear progression of the impedance real values as temperature decreases, as shown in Fig. 6, suggests that a higher-order polynomial model can be a good fit to the regression analysis. A quadratic regression analysis was applied to the experimental results in a similar process as the linear regression analysis. The quadratic model has the form $\hat{T} = \beta_1 R^2 + \beta_2 R + \epsilon$ where β_1 , β_2 and ϵ are the polynomial coefficients. Fig. 8 shows the fitted quadratic models along with the impedance measurement. The figure shows that at higher frequencies (> 200 Hz), the quadratic model shows a

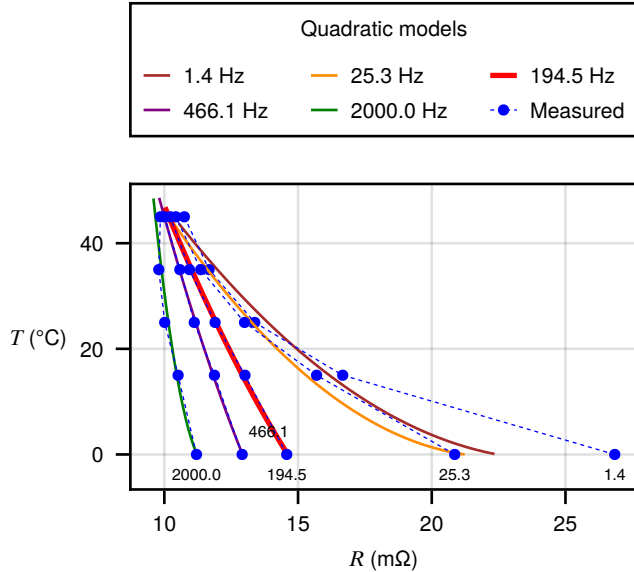


Fig. 8: Quadratic model fitting between the cell temperature and the real part of the measured impedance at various frequencies of cell C4 at 80% SOC.

SOC	20%	30%	40%	50%	60%	70%	80%
0 °C	1.4	1.32	1.34	0.81	0.61	1.32	0.77
15 °C	3.49	1.59	1.91	1.39	1.61	2.87	1.81
25 °C	4.09	4.25	3.09	2.92	2.82	3.15	2.43
35 °C	3.85	3.34	2.76	2.47	2.57	2.68	2.61
45 °C	0.8	0.9	0.84	1.02	0.87	1.07	0.91

TABLE II: Estimation errors (in degrees Celsius) of quadratic regression at various temperatures and SOCs.

good fit to the temperature-impedance relationship. Self validation yields significantly higher R^2 index and lower RMSE values at a wider range of frequencies compared to linear regression. Therefore, it was possible to lower the maximum RMSE criterion (< 2.5 °C) when identifying the optimal frequency range. A single harmonic frequency of 194.5 Hz was chosen as the final optimal estimator. The estimation errors obtained by applying the trained quadratic estimator on the test cell C1 are shown in Table I. On average, quadratic regression produced an estimation error of about 1.7 °C.

While the cell internal impedance has demonstrated a strong correlation to temperature, impedance values also have a strong dependency to other state parameters of the cell such as the SOC and the SOH. As the cells applied in this experimental work are new cells, the SOH can be assumed to be at cyclic age zero. Since the impedance values change according to the changes in SOC, it is necessary to re-apply the regression analysis process to the cell impedance measured at different SOC points. Table II shows the estimation errors of quadratic regression applied to the test cell C1 at various temperatures

and SOCs. The results show that temperature estimation accuracy varies depending on both SOC and temperature. Room temperature condition shows the most inaccuracies while either low or high temperature conditions show highly accurate estimation results.

VI. CONCLUSIONS

The temperature is a critical parameter which heavily influences safety and performance of Li-ion batteries. Studies have shown a strong relationship between the battery impedance and battery temperature. The recently proposed DIBS technique can be applied to quickly and accurately measure the battery impedance from which the temperature of a battery cell can be directly estimated without relying on temperature sensors or complicated modeling techniques.

This paper has demonstrated the application of the battery impedance measured using the DIBS method in determining the temperature of a Li-ion battery cell. Experimental measurements were carried out and analyzed to show the effectiveness of the method. Temperature estimation errors ranging between 0.7 °C and 4.5 °C have been obtained by applying regression techniques to a wide temperature interval ranging from 0 °C to 45 °C. The estimation performance varies depending on the cell temperature and SOC.

REFERENCES

- [1] G. Zubi et.al, "The lithium-ion battery: State of the art and future perspectives," *Renewable and Sustainable Energy Reviews*, vol. 89, pp. 292–308, 2018.
- [2] A. Jinasena et.al, "Online internal temperature sensors in lithium-ion batteries: State-of-the-art and future trends," *Frontiers in Chemical Engineering*, vol. 4, p. 804704, 2022.
- [3] M. C. et.al, "Use of impedance spectroscopy for the estimation of li-ion battery state of charge, state of health and internal temperature," *Journal of the Electrochemical Society*, vol. 168, no. 8, p. 080517, 2021.
- [4] J. Sihvo, D.-I. Stroe, T. Messo, and T. Roinila, "Fast approach for battery impedance identification using pseudo-random sequence signals," *IEEE transactions on power electronics*, vol. 35, no. 3, pp. 2548–2557, 2019.
- [5] E. Locorotondo, S. Scavuzzo, L. Pugi, A. Ferraris, L. Berzi, A. Airale, M. Pierini, and M. Carello, "Electrochemical impedance spectroscopy of li-ion battery on-board the electric vehicles based on fast nonparametric identification method," in *Proc. IEEE International Conference on Environment and Electrical Engineering and IEEE Industrial and Commercial Power Systems Europe*, 2019, pp. 1–6.
- [6] A. Fairweather, M. Foster, and D. Stone, "Battery parameter identification with pseudo random binary sequence excitation (prbs)," *Journal of Power Sources*, vol. 196, no. 22, pp. 9398–9406, 2011.
- [7] M. Tran and T. Roinila, "Online impedance measurement of lithium-ion battery: Applying broadband injection with specified fourier amplitude spectrum," *IEEE Transactions on Industry Applications*, 2023.
- [8] A. Y. Kallel, A. Fischer, and O. Kanoun, "Discrete interval binary sequence for stable and stationary impedance spectroscopy of li-ion batteries," *IEEE Transactions on Instrumentation and Measurement*, 2023.
- [9] X. Wang, X. Wei, J. Zhu, H. Dai, Y. Zheng, X. Xu, and Q. Chen, "A review of modeling, acquisition, and application of lithium-ion battery impedance for onboard battery management," *eTransportation*, vol. 7, pp. 1–21, 2021.
- [10] H. Beelen, L. Raijmakers, M. Donkers, P. Notten, and H. Bergveld, "A comparison and accuracy analysis of impedance-based temperature estimation methods for li-ion batteries," *Applied Energy*, vol. 175, pp. 128–140, 2016.
- [11] R. R. Richardson and D. A. Howey, "Sensorless battery internal temperature estimation using a kalman filter with impedance measurement," *IEEE Transactions on Sustainable Energy*, vol. 6, no. 4, pp. 1190–1199, 2015.

- [12] N. S. Spinner, C. T. Love, S. L. Rose-Pehrsson, and S. G. Tuttle, "Expanding the operational limits of the single-point impedance diagnostic for internal temperature monitoring of lithium-ion batteries," *Electrochimica Acta*, vol. 174, pp. 488–493, 2015.
- [13] J.-q. Li, L. Fang, W. Shi, and X. Jin, "Layered thermal model with sinusoidal alternate current for cylindrical lithium-ion battery at low temperature," *Energy*, vol. 148, pp. 247–257, 2018.
- [14] R. R. Richardson, P. T. Ireland, and D. A. Howey, "Battery internal temperature estimation by combined impedance and surface temperature measurement," *Journal of Power Sources*, vol. 265, pp. 254–261, 2014.
- [15] H. Beelen, L. Rajmakers, M. Donkers, P. Notten, and H. Bergveld, "An improved impedance-based temperature estimation method for lithium-ion batteries," *IFAC-PapersOnLine*, vol. 48, no. 15, pp. 383–388, 2015.
- [16] J. P. Schmidt, S. Arnold, A. Loges, D. Werner, T. Wetzel, and E. Ivers-Tiffée, "Measurement of the internal cell temperature via impedance: Evaluation and application of a new method," *Journal of Power Sources*, vol. 243, pp. 110–117, 2013.
- [17] D. D. Macdonald, "Reflections on the history of electrochemical impedance spectroscopy," *Electrochimica Acta*, vol. 51, no. 8-9, pp. 1376–1388, 2006.
- [18] A. V. D. BOS and R. Krol, "Synthesis of discrete-interval binary signals with specified fourier amplitude spectra," *International Journal of Control*, vol. 30, no. 5, pp. 871–884, 1979.
- [19] M. Buckner and T. Kerlin, "Optimum binary signals for reactor frequency response measurements," *Nuclear Science and Engineering*, vol. 49, no. 3, pp. 255–262, 1972.
- [20] K.-D. Paehlike and H. Rake, "Binary multifrequency signals - synthesis and application," *IFAC Proceedings Volumes*, vol. 12, no. 8, pp. 589–596, 1979.
- [21] S. L. Harris and D. A. Mellichamp, "On-line identification of process dynamics: use of multifrequency binary sequences," *Industrial & Engineering Chemistry Process Design and Development*, vol. 19, no. 1, pp. 166–174, 1980.